Nature Environment and Pollution Technology
An International Quarterly Scientific Journal

p-ISSN: 0972-6268
(Print copies up to 2016)
e-ISSN: 2395-3454

Vol. 21 | No. 1 | pp. 11-20 | 2022

Original Research Paper

https://doi.org/10.46488/NEPT.2022.v21i01.002

Open Access Journal

Effect on Soil Hydrodynamic Parameters in Fields Mulched with Gravel for Different Periods of Time

Wenju Zhao*†, Yali Wang*, Zongli Li and Taohong Cao***

*College of Energy and Power Engineering, Lanzhou University of Technology, Lanzhou 730050, China

**General Institute for Water Resources and Hydropower Planning and Design, Ministry of Water Resources, Beijing 100120, China

†Corresponding author: Wenju Zhao; wenjuzhao@126.com

Nat. Env. & Poll. Tech.
Website: www.neptjournal.com

Received: 23-02-2021
Revised: 27-04-2021
Accepted: 01-05-2021

Key Words:
Gravel mulched fields
Soil-water characteristics
Soil hydrodynamics

ABSTRACT

Soil-water characteristic curve (SWCC) and soil hydraulic conductivity are important soil hydrodynamic parameters, which are of great significance in production practice. In 128 soil samples collected from 0-20, 20-40 cm layers at sampling scales of 32×32 m, the authors determined the effect of different periods of time on SWCC and soil hydraulic conductivity in fields mulched gravel. The water holding capacity of soil changes dramatically throughout time, with NEW having the maximum water holding capacity. As the planting time increases, the soil water holding capacity decreases. Both van Genuchten (VG) and Gardner models can fit SWCC in different time periods well, but the fitting accuracy of the VG model is higher. Geostatistics and Kriging interpolation are used to study the spatial variability of the VG model parameters of the SWCCs. The parameters θ_s, α, and n show a strong spatial correlation as a whole and are slightly affected by random factors. The changing trend of soil unsaturated hydraulic conductivity ($K(\theta)$) in gravel-mulched fields is faster than the CHECK, and the NEW has the fastest change trend. The data suggest that fields mulched with gravel retain more water, with the NEW having the most noticeable water retention effect. The study's findings can be used to investigate the regional variations in soil hydrodynamic characteristics in gravel mulched fields in arid locations.

INTRODUCTION

Soil is not only the basis of sustainable agricultural development but also the environmental resources on which mankind depends for survival (Russo et al. 2015, Ren et al. 2018). The soil-water characteristic curve (SWCC) and soil hydraulic conductivity are significant factors for describing soil qualities that are crucial in production (Kishné et al. 2017, Pannecoucke et al. 2019). SWCC is the basic characteristic curve for studying soil water holding capacity, which can provide a scientific basis for studying the mechanism analysis and numerical simulation of water flow in the soil-plant-atmosphere continuum (SPAC system) (Raghuram et al. 2020). Soil hydraulic conductivity is of great significance in farmland irrigation and drainage and soil and water conservation projects (Fang et al. 2016). It has considerable spatial variability, which is mainly related to soil texture, structure, bulk density, nutrients, salinity, and organic matter content, and not simply represents the features of soil infiltration and leakage (She et al. 2014). The importance of studying soil hydrodynamic characteristics for agricultural productivity and soil moisture management cannot be overstated.

Many researchers have looked into the temporal and geographical variability of soil hydraulic parameters and discovered that they are linked to soil texture and structure. The majority of SWCC research focuses on the model's applicability (Dong et al. 2017, Zhao et al. 2020a) and geographical variability (Xing et al. 2015, Shi et al. 2014). Zhao et al. (2020a) investigated the SWCC model in gravel-covered fields in Northwest China and discovered that the van Genuchten (VG) model fits well and is more accurate in predicting soil moisture. According to Wang et al. (2015b), the SWCC is influenced by elements like soil texture and structure, and due to the heterogeneity of these components, the SWCC undergoes significant changes over time and space (Amanabadi et al. 2018). The saturated permeability of the soil is measured by soil hydraulic conductivity, which is also an important parameter in the hydrological model (Mao et al. 2019). Yu et al. (2018) investigated the spatial distribution characteristics of saturated hydraulic conductivity of different soil layers at the regional scale of the loess area using classical statistics and geostatistics and discovered that soil hydraulic conductivity gradually decreased with increasing soil depth. Li et al. (2019) investigated the regional variability of soil hydraulic parameters in Xinjiang and discovered that soil hydraulic conductivity has a considerable spatial dependence.

For more than 300 years, many lands in Northwest China's arid and semi-arid regions have been covered with

gravel and sand as a "no-tillage protection scheme" (Li 2003, Zhao et al. 2017a). This model can effectively reduce surface runoff, increase water infiltration rate, reduce evaporation, and have a thermal insulation effect (Li 2003, Qiu et al. 2014, Zhao et al. 2020b). Many countries with precipitation < 400 mm have applied various patterns of sandstone coverage (Modaihsh et al. 1985, Kemper et al. 1994). However, due to human or natural reasons, this kind of land will degenerate after several years of planting (Wang et al. 2010), causing the interface between the gravel and the soil layer to become unclear. The influence and interaction of various processes in the soil profile of this soil at different periods can produce variable soils (Harguindeguy et al. 2018).

However, most scholars are concerned about the spatial change of a single soil property. Little attention has been paid to the changing laws of hydraulic parameters of soil mulched with gravel. The objectives of the study are to (1) compare and analyze the change laws of SWCCs in different periods, obtain changing laws of soil water holding capacity of fields mulched with gravel at different planting periods, and use VG and Gardner empirical models to fit the SWCCs and analyze the VG model parameters and determine its spatial statistical characteristics, and (2) analyze the differences of soil hydraulic conductivity at different depths in fields mulched with gravel for different periods of time. By examining changes in soil hydrodynamic characteristics in fields mulched with gravel over different lengths of time in the arid area of Northwest China, it is expected to provide theoretical support for soil moisture management and crop planting benefits of fields mulched with gravel. Our findings have important significance for small-scale hydrological studies in the sand and gravel-covered arid and semi-arid areas.

MATERIALS AND METHODS

Description of the Study Area and Sample Collection

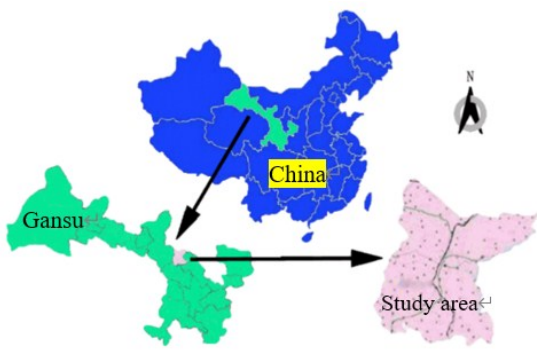

Fig. 1: Study area and the soil sampling locations in the study area situated in Gansu, China.

The study was conducted in Jingtai County near the Lanzhou University of Technology experimental station in the middle of the western portion of China's Gansu province (on the east side of the Hexi corridor, at the junction of provinces (regions) of Gansu, Ningxia, and Inner Mongolia) (Fig. 1). The planting area of gravel mulched field in the study area occupies an area of approximately 33.3 km^2. The climate is intermediate between continental monsoon and non-monsoon regions. The temperature fluctuates from -27.3 to 36.6°C from the winter to summer seasons, with a mean annual temperature of 8.2°C. The mean annual precipitation is 185 mm, with a rainy season (accounting for approximately 61.4% of the annual rainfall) from July to September. The mean annual evaporation is 3038 mm, with annual average evaporation to precipitation ratio of 16 (Wu et al. 2019). The predominant soils are sandy loam, and the particles size was classified into three grades: clay (0-0.002 mm), silt (0.002-0.05 mm), and sand (0.05-2 mm), following the USDA Soil Taxonomy (Table 1).

The fields were 32×32 m and consisted of a new field mulched with gravel (NEW) planted for less than 10 years, a moderately aged field mulched with gravel (MOD) planted for 25-30 years, an old field mulched with gravel (OLD) planted for 45-60 years and bare land (no vegetation or gravel) as a control (CHECK). The surface sand was carefully removed, and all samples were then collected using stainless-steel cutting rings (5 cm in height by 5 cm in diameter) from the 0-20 and 20-40 cm layers. The samples were collected from the two layers in 64 evenly distributed 1×1 m quadrats 4 m apart, center to center, for a total of 128 samples (Fig. 2). Saturated hydraulic conductivity was determined by the constant-head method using a constant-head permeation apparatus (TST-70, China). Data for constructing SWCCs were obtained using a Hitachi CR21 high-speed constant-temperature refrigerated centrifuge (Vero et al. 2016).

Analysis Methods

Soil saturated hydraulic conductivity, K_s (mm/min), was calculated by:

$$K_s = \frac{V_s}{I} \quad \ldots(1)$$

where V_s is the infiltration rate and I is the water pressure gradient.

The van Genuchten model is:

$$\theta(h) = \theta_r + \frac{\theta_s - \theta_r}{(1+|\alpha h|^n)^m} \quad \ldots(2)$$

where θ is volumetric water content ($cm^3.cm^{-3}$), θ_s is saturated volumetric water content (cm^3/cm^3), θ_r is residual

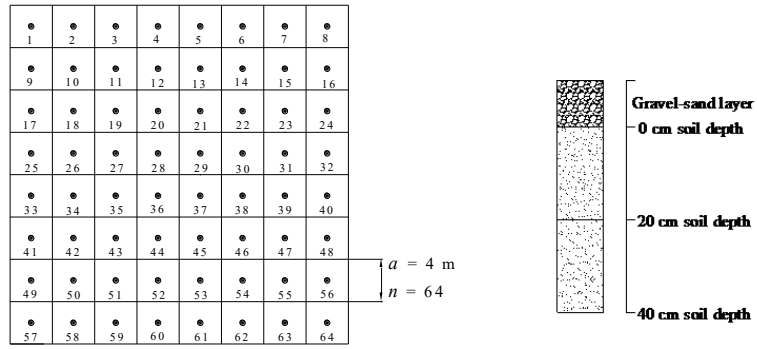

Note: *a* is the grid-scale and *n* is the total number of sampling points.

Fig. 2: Distribution map of the sampling points.

volumetric water content ($cm^3.cm^{-3}$), *h* is the pressure head (m), α is a scaling parameter that is inversely proportional to mean pore diameter, and *m* and *n* are shape coefficients, where *m* and *n* are related, *m*=1-1/*n*.

The Gardner model is:

$$lg\, h = - A lg\, \theta - B \quad \ldots(3)$$

where *A* and *B* are empirical parameters >0, with a linear relationship.

K*(θ)* is the unsaturated hydraulic conductivity of the soil (mm.min¯1). It is a function of soil water content and soil suction, and increases with SWC and decreases as soil suction increases (Wang et al. 2012). The hydraulic conductivity model for unsaturated soil is (van Genuchten et al. 1980):

$$K(\theta) = K_s \left(\frac{\theta - \theta_r}{\theta_s - \theta_r} \right)^{1/2} \left[1 - \left(1 - \left(\frac{\theta - \theta_r}{\theta_s - \theta_r} \right)^{1/m} \right)^m \right]^2 \quad \ldots(4)$$

Based on the regionalized variables theory and intrinsic hypothesis, the semivariogram, $\gamma(h)$, was estimated by:

$$\gamma(h) = \frac{1}{2N(h)} \sum_{i=1}^{N(h)} \left[Z(x_i + h) - Z(x_i) \right]^2 \quad \ldots(5)$$

where $N(h)$ is the number of pairs of observations ($Z(x_i)$ and $Z(x_i+h)$) separated by a distance *h*. Only isotropic semivariograms are considered.

The following is the equation of the Kriging interpolation method:

$$Z(x_0) = \sum_{i=1}^{n} \lambda_i Z(x_i) \quad \ldots(6)$$

Where $Z(x_0)$ is the estimated value at point x_0, *n* is the number of known points around the point to be estimated, λ_i is the weight of each sample, and $Z(x_i)$ is the sample value at point x_i.

The coefficient of determination (R^2) between measured and predicted values and root mean square error (RMSE) was used to evaluate the performance of the regression models as follows:

Table 1: Basic nature of the various layers of the fields.

Test Soil	Soil Depth [cm]	Clay [%]	Silt [%]	Sand [%]	K_s[mm/min]
		<0.002 mm	0.002-0.05 mm	0.05-2 mm	
NEW	0-20	2.42	55.15	42.44	0.48
	20-40	2.74	55.35	41.92	0.46
MOD	0-20	2.59	53.94	43.48	0.44
	20-40	2.93	53.25	43.83	0.41
OLD	0-20	2.65	60.44	36.92	0.42
	20-40	3.15	65.41	31.45	0.38
CHECK	0-20	2.82	53.67	43.52	0.36
	20-40	3.32	55.93	40.76	0.33

$$R^2 = \left[\frac{\sum_{i=1}^{n}(O_i - \overline{O})(P_i - \overline{P})}{\left[\sum_{i=1}^{n}(O_i - \overline{O})^2\right]^{0.5}\left[\sum_{i=1}^{n}(P_i - \overline{P})^2\right]^{0.5}} \right]^2 \quad \ldots(7)$$

$$RMSE = \sqrt{\frac{\sum_{i=1}^{n}(P_i - O_i)^2}{n}} \quad \ldots(8)$$

where O_i and P_i are the measured and predicted values, respectively, $\overline{O}$ and $\overline{P}$ are the average measured and predicted values, respectively, and n is the number of observations in the validation data set. Both R^2 and RMSE range from 0 to 1. A high $R^2$and a low RMSE indicate high predictive accuracy (Zhang et al. 2012).

RESULTS AND DISCUSSION

Influence of Different Periods of Time on SWCCs

The relationship between soil water content (SWC) and soil suction was established by characterizing dehydration (Fig. 3). The SWCCs of different soil layers at different time periods are consistent. In the low suction phase (<1 bar), the SWC of different soil layers at different time periods decreases rapidly with the increase of suction, while in the intermediate and high suction phases (1-10 bar), the SWC at different periods of time decreases slowly with the increase of suction. The SWC is 20-40 cm> 0-20 cm when the soil suction is the same. The capacity of the soil to hold water differed greatly between times. The NEW had the most capacity for water storage. The soil water holding capacity decreased as the planting time increased, and the CHECK was the lowest. This is because as the number of planting years increases, the amount of sand and gravel particles in the soil increases. Compared with the CHECK, the mixing coarser particles in the soil reduces the total porosity of the soil, resulting in a gradual decrease in soil water holding capacity (Udawatta et al. 2008).

Fitting of SWCCs for Different Periods of Time

The VG model and Gardner model were used to fit the SWCCs at different periods of time, and the error analysis of the measured and predicted SWC under different suction was performed (Table 2). The fitting results reveal that the predicted value of SWC is similar to the measured value, with an R^2 value of 0.990-0.997 and an RMSE of 0.080-0.086. The VG model is built on *RETC* software to parameterize SWCCs. The Gardner model, which was fitted using Origin 2019b, has a lower R^2 and RMSE than the VG model. The VG model may be used to fit SWCCs in fields mulched with gravel for various periods of time due to its improved accuracy; the results were compatible with Fu et al. (2011).

The tested soil type in this experiment is sandy loam, the θ_r fitted by *RETC* software is very low and almost close to zero, so this paper only discusses the θ_s, α, and n. The effect of different planting years on the SWCCs parameters in fields mulched gravel also has certain differences. θ_s and α are significantly affected, and the influence on n is small. Planting years have a great impact on the physical properties of the soil, which is reflected in the impact of different planting years on the saturated soil moisture content. The θ_s of fields mulched gravel is higher than CHECK, and NEW is the highest. The α is the reciprocal of the air intake value. The air intake value of NEW is the largest, and that of CHECK is the smallest. The results show that the NEW has the best soil structure compared to CHECK, which is conducive to the escape of air inside the structure and increases the saturation of soil moisture to a certain extent. The change of the empirical parameter n in different planting years is relatively

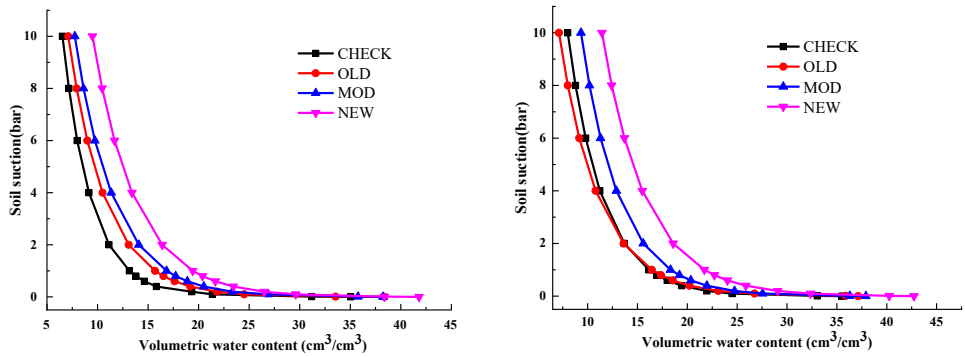

(a) 0-20 cm (b) 20-40 cm

Fig. 3: The SWCCs of fields mulched with gravel for different periods of time.

Table 2: Fitting values and fitting errors of hydraulic parameters with VG and Gardner models.

Test Soil	Soil Depth [cm]	VG Model					Gardner Model			
		θ_s	α	n	R^2	*RMSE*	*A*	*B*	R^2	*RMSE*
NEW	0-20	0.406	2.447	1.242	0.993	0.085	4.543	2.396	0.942	0.212
	20-40	0.418	1.948	1.229	0.995	0.086	4.989	2.465	0.942	0.213
MOD	0-20	0.376	2.567	1.260	0.995	0.084	4.187	2.399	0.946	0.205
	20-40	0.378	2.476	1.234	0.995	0.081	4.731	2.639	0.951	0.195
OLD	0-20	0.371	3.977	1.247	0.990	0.083	4.144	2.501	0.944	0.208
	20-40	0.369	2.167	1.277	0.995	0.084	3.949	2.265	0.940	0.214
CHECK	0-20	0.346	5.875	1.244	0.997	0.083	4.257	2.851	0.975	0.139
	20-40	0.350	3.100	1.236	0.994	0.080	4.567	2.769	0.952	0.191

Table 3: Theoretical Model and Parameters of Semi-variance Function.

Hydraulic Parameters	Test Soil	Soil Depth [cm]	Theoretical model	C_0 [10^{-3}]	C_0+C [10^{-3}]	A_0	C_0/C_0+C	R^2
θ_s	NEW	0-20	Exponential	0.0049	0.050	7.62	0.098	0.733
		20-40	Gaussian	0.0234	0.248	58.73	0.094	0.918
	MOD	0-20	Exponential	0.1250	0.495	70.00	0.253	0.738
		20-40	Linear	0.6265	0.626	29.20	1.000	0.755
	OLD	0-20	Exponential	0.0023	0.026	5.61	0.089	0.821
		20-40	Spherical	0.0005	0.013	7.02	0.035	0.726
	CHECK	0-20	Spherical	0.0003	0.014	6.86	0.021	0.763
		20-40	Exponential	0.0106	0.033	71.00	0.032	0.708
α	NEW	0-20	Exponential	0.0004	0.005	6.81	0.080	0.757
		20-40	Gaussian	0.0001	0.201	58.90	0.0004	0.955
	MOD	0-20	Gaussian	0.6503	5.77	57.99	0.113	0.956
		20-40	Linear	0.6256	0.626	29.20	1.000	0.830
	OLD	0-20	Linear	0.0190	0.019	29.20	1.000	0.742
		20-40	Exponential	0.0214	0.063	71.00	0.341	0.741
	CHECK	0-20	Exponential	0.0160	0.194	7.08	0.082	0.740
		20-40	Linear	0.0150	0.015	29.20	1.000	0.785
n	NEW	0-20	Gaussian	0.0410	0.360	110.70	0.114	0.943
		20-40	Exponential	0.0208	0.145	4.18	0.143	0.753
	MOD	0-20	Exponential	0.2650	0.765	71.00	0.346	0.806
		20-40	Gaussian	29.3000	139.100	59.92	0.211	0.748
	OLD	0-20	Linear	0.1220	0.122	29.20	1.000	0.774
		20-40	Linear	0.0580	0.058	29.20	1.000	0.781
	CHECK	0-20	Exponential	0.0083	0.082	9.00	0.101	0.821
		20-40	Linear	0.0200	0.020	29.20	1.000	0.958

stable, between 1.229 and 1.277. Except for the OLD, n decreases with the increase of soil depth. This is consistent with the results of Gao et al. (2014) on the spatial variability of SWCCs under different fertilization.

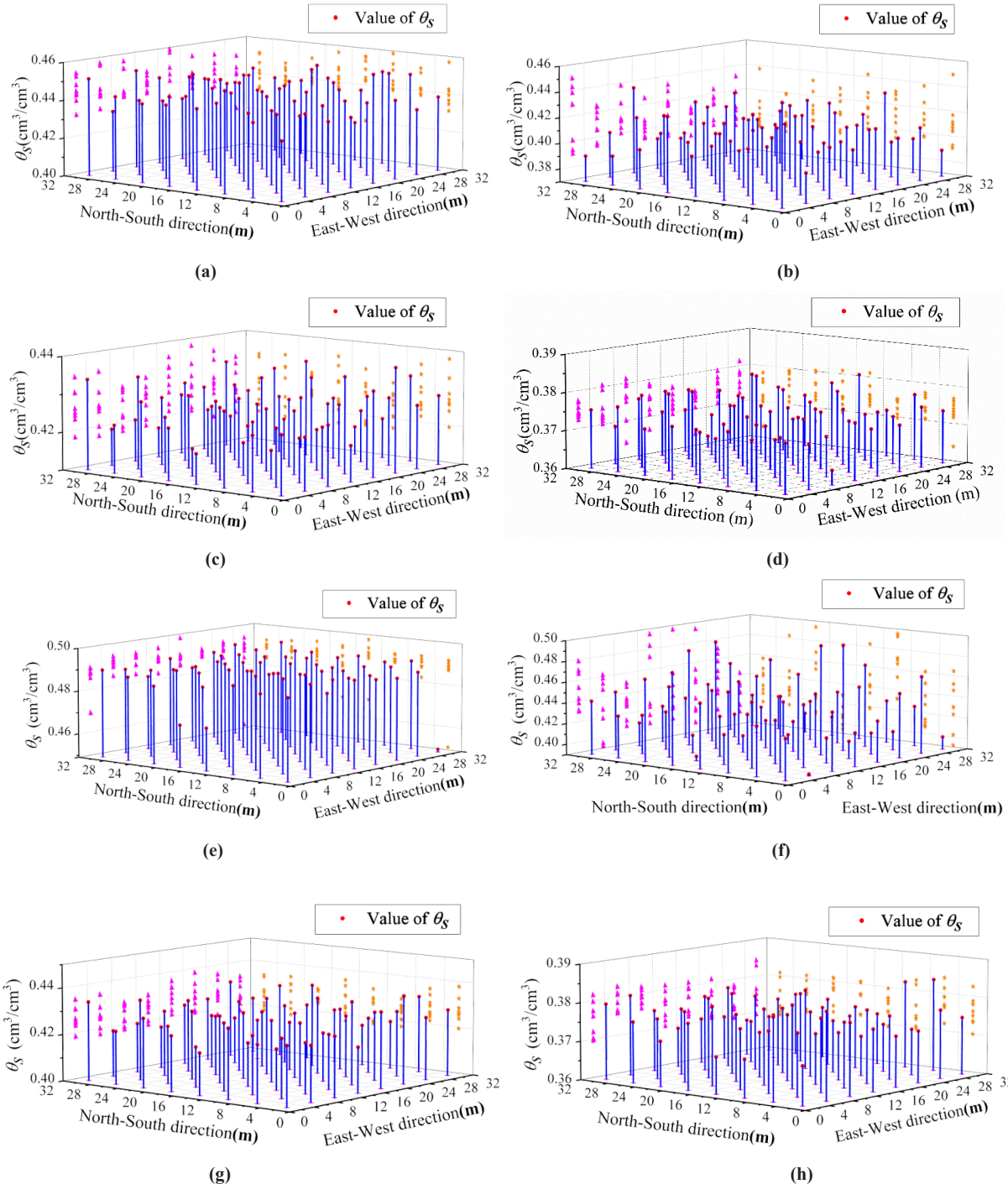

Fig. 4: Trend surface analysis of θ_s: (a) NEW: 0-20cm; (b) MOD: 0-20cm; (c) OLD: 0-20cm; (d) CHECK: 0-20cm; (e) NEW: 20-40cm; (f) MOD: 20-40cm; (g) OLD: 20-40cm; (h) CHECK: 20-40cm.

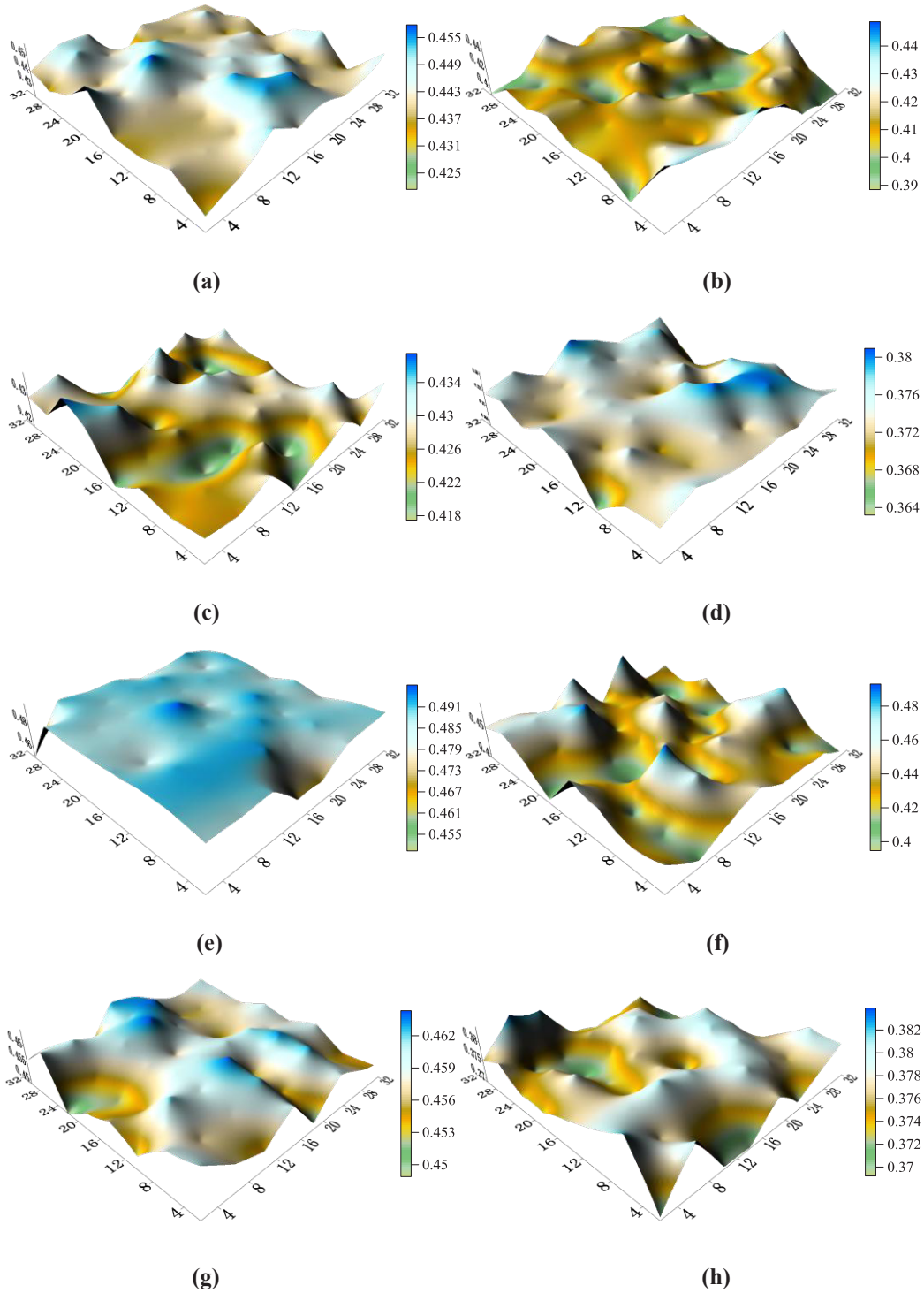

Fig. 5: Distribution maps of θ_s predicted by Kriging: (a) NEW: 0-20cm; (b) MOD: 0-20cm; (c) OLD: 0-20cm; (d) CHECK: 0-20cm; (e) NEW: 20-40cm; (f) MOD: 20-40cm; (g) OLD: 20-40cm; (h) CHECK: 20-40cm.

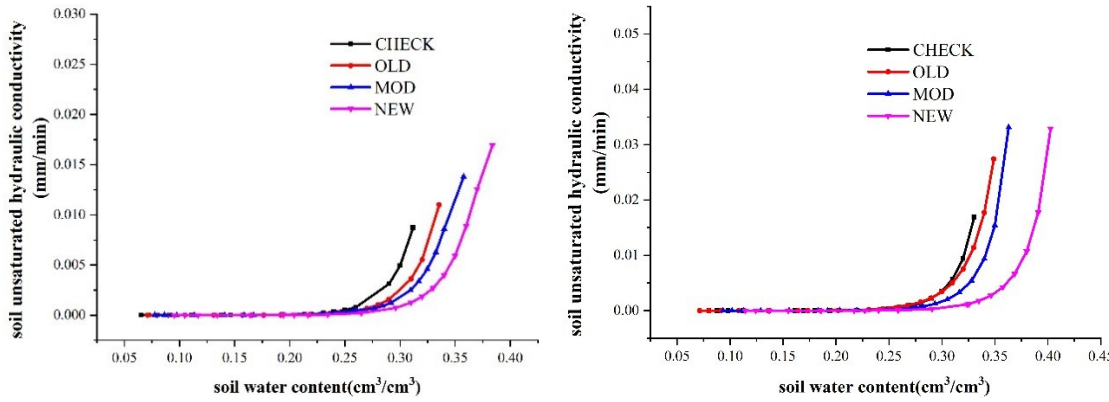

Fig. 6: Curves for soil hydraulic conductivity in (a) 0-20 cm; (b) 20-40 cm layer.

Geostatistical Analysis of VG Model Parameters

To analyze the spatial variability of the VG model parameters of each soil layer for different periods of time, the θ_s, α and n were analyzed by semi-variance using *GS+9.0* software, and the spatial variability function model parameters and regression model test parameters were obtained (Table 3). The results of the spatial variability analysis of the VG model parameters show that the θ_s, α, and n can be fitted with Gaussian, Linear, and Exponential models, and the Gaussian model has higher accuracy. The average values of nugget values (C_0) of θ_s, α, and n are $0.099*10^{-3}$, $0.168*10^{-3}$, and $3.729*10^{-3}$, respectively. Except for the large change of n in MOD, the C_0 of other test soil types are relatively stable and the degree of change is small, indicating that the degree of spatial variation is caused by random factors such as soil characteristics, sampling, or measurement errors is small. The variable range (A_0) is larger than the sampling interval of 4 m, indicating that the selected model is ideal and can reflect the spatial correlation of the parameters of the soil moisture characteristic curve. For θ_s, α, and n, most of the nugget variance values $C_0/(C_0+C)$ are less than 0.25, only a few $C_0/(C_0+C)$ values are between 0.25-1, indicating that the θ_s, α, and n in the 0-40cm soil layer show strong spatial correlation (Cambardella et al.1994), and the overall degree of variation of random factors is small, which means the spatial heterogeneity caused by the spatial variability of soil structure is the dominant factor. This is consistent with the results of studies such as Xing et al. (2014), even if multi-point sampling is used to determine the SWCC on a small scale, it will inevitably exhibit different spatial distribution characteristics. Zhu et al. (2003) showed that the spatial variability of VG model parameters is related to soil texture, organic matter content, and bulk density.

Spatial Distribution of VG Model Parameters

The combination of trend surface analysis (Fig. 4) and Kriging interpolation (Fig. 5) can more intuitively reflect the spatial distribution characteristics of VG model parameters. In this study, we used distribution characteristics of θ_s as examples. Each blue vertical line in Fig. 4 represents the θ_s value of a sampling point. These points are projected on the orthogonal plane of the East-west direction and North-south direction. The spatial distribution of θ_s in 0-20 cm and 20-40 cm soil layers of different periods of time have obvious patches and stripes. The distribution area of high-value areas in NEW, MOD, and OLD is significantly larger than CHECK. Compared with CHECK, the projection points of the θ_s of the NEW are most concentrated, while the distribution of the θ_s of the MOD and the OLD is relatively scattered, indicating that with the increase of planting years, the fields mulched with gravel will be more affected by random factors.

As shown in Fig. 5, the θ_s of each SWCC present a "bump" and "sag". The distribution of θ_s in NEW is relatively "flat", indicating that θ_s in NEW have strong spatial autocorrelation, and the spatial heterogeneity caused by spatial autocorrelation is greater than that caused by random factors. The θ_s of CHECK have obvious "bump and sag", which indicates that the θ_s of CHECK is greatly affected by random factors, which further proves that the water retention of fields mulched with gravel is better. The number of bumps decreases with increasing depth, which may be related to the irregular surface topography of the

study area, and tends to stabilize with increasing depth (Zhao et al. 2017b).

Comparative Analysis of $K(\theta)$ with Different Periods of Time

Substituting the fitting parameter values of the VG model in Table 3 and the values of K_s from Table 1 in Eq. (4), the $K(\theta)$ formulas of tested soils are obtained. With $K(\theta)$ as the ordinate and the volume SWC as the abscissa, plot the $K(\theta)$ curves of 0-20 cm and 20-40 cm soil layers in different planting years (Fig. 6). When the SWC is close to saturation, the four types of $K(\theta)$ curves all have an inflection point showing a sharp vertical upward trend. Before the inflection point, the $K(\theta)$ curves are almost parallel to the horizontal axis, indicating that the $K(\theta)$ has become stable and close to 0. The abrupt inflection point of the $K(\theta)$ curves are mainly caused by the different soil water suction and the different connectivity of the water in the soil pores (Wang et al. 2015a). When the $K(\theta)$ is the same, the SWC of the fields mulched with gravel is greater than that of the CHECK, indicating that the water-holding capacity of the fields mulched with gravel is better than that of the CHECK.

When the $K(\theta)$ is the same, the changing trend of water content at different depths is NEW > MOD > OLD > CHECK. The large-pore structure of the soil in the mulched fields was destroyed as period of gravel mulching increased. According to She et al. (2014) showed that SWC and friction during the outflow were also large, so $K(\theta)$ curve is highest for OLD.

CONCLUSIONS

The authors of this paper examined SWCCs in fields mulched with gravel for different periods of time and discovered that the soil water retention capacity varies substantially. The NEW has the highest capacity for water holding. The soil water holding capacity decreases as planting time advances, and the CHECK is at its lowest. The results of fitting the SWCCs with the VG model and the Gardner model show that the VG model has a higher fitting accuracy. Geostatistics and Kriging interpolation are used to study the spatial variability of the VG model parameters. The nugget coefficient values $C_0/(C_0+C)$ of the θ_s, α, and n are mostly less than 0.25, showing a strong spatial correlation overall. It can be seen from the spatial distribution map of θ_s in the OLD are "high" and "sag", while the distribution map of the NEW is relatively "flat". The changing trend of $K(\theta)$ of fields mulched gravel is faster than that of CHECK, and the changing trend of NEW is the fastest.

ACKNOWLEDGMENTS

This research was supported by the National Natural Science Foundation of China (51869010), Guidance Program for Industrial Support of Colleges and Universities in Gansu Province (2019C-13), Longyuan Youth Innovation and Entrepreneurship Project, and the Lanzhou University of Technology Hongliu first-class discipline funding.

REFERENCES

Amanabadi, S., Mohammadi, M.H. and Masihabadi, M.H. 2018. Predicting continuous form of soil-water characteristics curve from limited particle size distribution data. Water SA, 44(3): 428-435.

Cambardella, C.A., Moorman, T.B. and Novak, J.M. 1994. Field-scale variability of soil properties in central Iowa soils. Soil. Sci. Soc. Am. J., 58(5): 1501-1511.

Dong, Y.Y., Zhao, C.Y. and Yu, Z.T. 2017. Characteristic curves and models analysis of soil water in interdune at the southern edge of Gurbantunggut Desert. J. Soil. Water. Conserv., 31(1): 166-171.

Fang, K., Li, H. and Wang, Z. 2016. Comparative analysis on spatial variability of soil moisture under different land-use types in the orchard. Sci. Hortic., 207: 65-72.

Fu, X.L., Shao, M.A. and Lu, D.Q. 2011. Soil water characteristic curve measurement without bulk density changes and its implications in the estimation of soil hydraulic properties. Geoderma, 167: 1-8.

Gao, H.Y., Guo, S.L. and Liu, W.Z. 2014. Spatial variability of soil water retention curve under fertilization practices in arid-highland of the Loess Plateau. Trans. Chin. Soc. Agric. Mach., 45(6): 161-165 and 176.

Harguindeguy, S., Pierre C. and Martine P.G. 2018. Colloidal mobilization from soil and transport of uranium in (sub)-surface waters. Environ. Sci. Pollut. Res., 26(2): 5294-5304.

Kemper, W., Nicks, A. and Corey, A.J. 1994. Accumulation of water in soils under gravel and sand mulches. Soil Sci. Soc. Am. J., 58(1): 56-63.

Kishné, A.S., Yimam, Y.T. and Morgan, C.L.S. 2017. Evaluation and improvement of the default soil hydraulic parameters for the Noah land surface model. Geoderma, 285: 247-259.

Li, X.D., Shao, M.A. and Zhao, C.L. 2019. Spatial variability and simulation of soil hydraulic parameters in arid northwest China. Arid Zone Res., 36(6): 1325-1332.

Li, X.Y. 2003. Gravel-sand mulch for soil and water conservation in the semiarid loess region of northwest China. Catena, 52(2): 105-127.

Mao, N., Huang, L.M. and Shao, M.G. 2019. Profile distribution of soil saturated hydraulic conductivity and controlling factors under different vegetations on a slope in the loess region. Soils, 51(2): 381-389.

Modaihsh, A.S., Horton, R. and Kirkham, D.J. 1985. Soil water evaporation suppression by sand mulches. Soil. Sci., 139(4): 357-361.

Pannecoucke, L., Le Coz, M. and Houzé, C. 2019. Impact of spatial variability in hydraulic parameters on plume migration within unsaturated surficial formations. J. Hydrol., 574: 160-168.

Qiu, Y., Wang, Y. and Xie, Z. 2014. Long-term gravel-sand mulch affects soil physicochemical properties, microbial biomass, and enzyme activities in the semi-arid Loess plateau of north-western China. Acta Agric. Scand. Sect. B., 64(4): 294-303.

Raghuram, A.S.S., Basha, B.M. and Moghal, A.A.B. 2020. Effect of fines content on the hysteretic behavior of water-retention characteristic curves of reconstituted soils. J. Mater. Civ. Eng., 32(4): 04020057.1-04020057.13.

Ren, C., Zhang, W. and Zhong, Z. 2018. Differential responses of soil microbial biomass, diversity, and compositions to altitudinal gradients depend on plant and soil characteristics. Sci. Tot. Environ., 610: 750-758.

Russo, G., Vivaldi, G.A. and De Gennaro B. 2015. Environmental sustainability of different soil management techniques in a high-density olive orchard. J. Cleaner Prod., 107: 498-508.

She, D.L., Liu, Y.Y. and Yu, S.E. 2014. Comparison of soil hydraulic properties under different land-use patterns. Trans. Chin. Soc. Agric. Mach., 45(9): 175-179 and 186.

Shi, W.J. Ma, Y. Xu F. 2014. Spatial variability of soil moisture and salt content in a cotton field on microscales under mulch drip irrigation Adv. Water Sci., 25 4 : 585-593.

Udawatta, R.P., Kremer, R.J. and Adamson, B.W. 2008. Variations in soil aggregate stability and enzyme activities in temperate agroforestry practice. Agric. Ecosyst. Environ., 39: 153-160.

Van Genuchten, M T. 1980. A closed-form equation for predicting the hydraulic conductivity of unsaturated soils. Soil Sci. Soc. Am. J., 44(5): 892-898.

Vero, S.E., Healy, M.G. and Henry, T. 2016. A methodological framework to determine optimum durations for the construction of soil water characteristic curves using centrifugation. Ir. J. Agric. Food Res., 55(2): 91-99.

Wang, H.L., Tang, X.Y. and Zhang, W. 2015a. Effects of biochar application on tilth soil hydraulic properties of slope cropland of purple soil. Trans. Chin. Soc. Agric. Eng., 4: 107-112.

Wang, J.N., Xie, Z.K. and Guo, Z.H. 2010. Simulating the effect of gravel-sand mulched field degradation on soil temperature and evaporation. J. Desert. Res., 30(2): 388-393.

Wang, P., Xie, C.J. and Chen, J. 2012. Degradation of sand fields and water-salt variations with different planting years. Bull. Soil Water Conserv., 32(2): 251-254.

Wang, Z.C., Li, X.Y. and Shi, H.B. 2015b. Effects of residual plastic film on soil hydrodynamic parameters and soil structure. Trans. Chin. Soc. Agric. Mach., 46(5): 101-106.

Wu, J., Liv, Y.N. and Li, C.B. 2019. Fine classification of county crops based on multi-temporal images of Sentinel-2A. Trans. Chin. Soc. Agric. Mach., 50(9): 194-200.

Xing, X.G., Zhao, W.G. and Liu, Y. 2015. Spatial variability of soil moisture in the kiwi field under different sampling density conditions. Trans. Chin. Soc. Agric. Mach., 46(8): 138-145.

Yu, D.X., Jia, X.X. and Huang, L.M. 2018. Spatial variation and influencing factors of saturated hydraulic conductivity in different soil layers of the loess area. Chin. J. Soil Sci., 49(5): 71-77.

Zhang, S.W., Huang, Y.F. and Shen, C.Y. 2012. Spatial prediction of soil organic matter using terrain indices and categorical variables as auxiliary information. Geoderma, 171(2): 35-43.

Zhao, W.J., Cao, T.H. and Li, Z.L. 2020a. Spatial variability of the parameters of soil-water characteristic curves in gravel-mulched fields. Water Sci. Technol., 20(1): 231-239.

Zhao, W.J., Cui, Z. and Zhang, J.Y. 2017a. Temporal stability and variability of soil-water content in a gravel-mulched field in northwestern China. J. Hydrol., 552: 249-257.

Zhao, W.J., Cui, Z. and Zhou, C.Q. 2020b. Spatiotemporal variability of soil–water content at different depths in fields mulched with gravel for different planting years. J. Hydrol., 590.

Zhao, W.J., Sheng, J. and Li, Z.L. 2017b. Spatial variability of soil salinity in a gravel-sand mulched jujube orchard at different scales. J. Irrig. Drain. Eng., 143: 0401700911-0401700918.

Zhu, A.N., Zhang, J.B., Chen X.M. et al. 2003. Study on Pedo-Transfer function in FENGQIU. Acta Pedol. Sin., 1: 53-58.